



FAU Institutional Repository

<http://purl.fcla.edu/fau/fauir>

This paper was submitted by the faculty of [FAU's Harbor Branch Oceanographic Institute](#).

Notice: ©1998 IEEE. Personal use of this material is permitted. Permission from IEEE must be obtained for all other uses, in any current or future media, including reprinting/republishing this material for advertising or promotional purposes, creating new collective works, for resale or redistribution to servers or lists, or reuse of any copyrighted component of this work in other works.

This manuscript is available at <http://ieeexplore.ieee.org/> and may be cited as: Caimi, F. M., Tongta, R., Carroll, M., & Murshid, S. (1998). Acoustic impulse response mapping for acoustic communications in shallow water. *Oceans '98: Conference proceedings: 28 September-1 October, 1998, Nice, France, Acropolis Convention Center*. (Vol. 3, pp. 1739-1743). Piscataway, NJ: Oceans '98 IEEE/OES Conference Organizing Committee. doi:10.1109/OCEANS.1998.726385

ACOUSTIC IMPULSE RESPONSE MAPPING FOR ACOUSTIC COMMUNICATIONS IN SHALLOW WATER

Frank M. Caimi, Rangan Tongta, Michael Carroll, Syed Murshid
 Department of Electrical Engineering/Engineering Division
 Harbor Branch Oceanographic Institution, Inc.
 5600 US 1 North
 Ft. Pierce, Florida 34946

Abstract -

In this paper we review the accepted methods for characterization of digital communications channels and present results from recent measurements made in shallow water. Several different methods for characterization are reported for signals over a frequency range of 40 to 60 kHz. The use of a system identification method (SID) for equalization of received data transmission is presented and compared to standard methodology for data rates to 10kbps. Comparison of OAIR derived from standard acoustic propagation models is also presented.

I. INTRODUCTION

The performance of underwater digital acoustic communications have improved with respect to data rate, bit error rate reduction, and adaptation to variations in the acoustic channel during the past decade [1-3]. Different architectures and multipath compensation schemes have been proposed and implemented using coherent and noncoherent modulation strategies. The inherently higher data rates achievable with coherent methods, such as m-ary PSK, for given carrier-to-noise ratios for given bit error rates in cooperative channels, have led to general acceptance in many applications areas. Equalizer and system performance are dependent upon relative stationarity of the channel during transmission intervals. In shallow water environments, interaction of the acoustic field with the surface or substrate can create significant channel variation. A variety of other effects, such as internal waves, reverberation, etc. may also be responsible for unreliable communications system performance.

In this paper, we examine several system architectures used for underwater acoustic communications and suggest measures for performance characterization. Performance criteria are related to acoustic parameters through simulation of the acoustic environment and by actual measurement. Results of simulations are given and compared using channel physical characteristics. A study of motion related effects between receiver/projector (or source) platform are presented. Adaptation characteristics under variable acoustic conditions are also covered for a reconfigurable receiver architecture using a *System Identification* (SID) approach. *Equalization using system identification* (EQSID) provides a direct method for estimation of the channel impulse response and/or channel model using received data prior to demodulation, and can

be used to track channel variations occurring at a fraction of the symbol rate.

II. THEORY

It has been shown that ocean acoustic channels are time variant with significantly rapid fluctuations such that frequent corrections for the channel impulse response are required [4]. Coherent communications transmission and reception systems require special concern when the channel is overspread; that is, when the product of the rms doppler spread and time spread is greater than one. This corresponds to variability that is within the symbol period in frequency. In benign acoustic environments, this condition may not be observed, suggesting the viability of coherent modulation methods and indeed these have been employed with success [1,4,5]. When the channel is stationary over successive symbol periods, adaptive filtering schemes are viable for correction of channel intersymbol interference.

A typical coherent communications receiver consists of an inner and outer structure. The outer receiver restructures input data via encoding and decoding so that optimum performance of the inner receiver structure shown in Fig. 1 is obtained.[6]

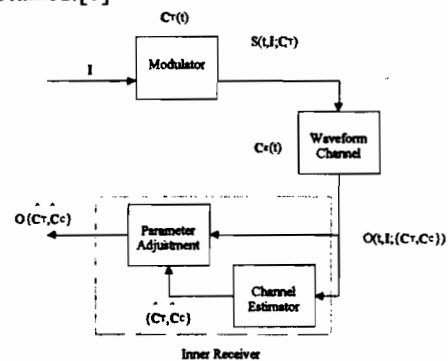


Fig. 1. Communication receiver inner structure.

From the point of view of information theory, the receiver maps a set of symbols into an input sequence $I = (i_1 \dots i_n)$, which is transmitted across the channel to yield an output sequence $R = (o_1 \dots o_n)$ that may be subsequently decoded into the original set of symbols. The actual input sequence is converted to a physical signal $s(t; I; C_r)$ by the modulator and is sent across the channel producing a distorted waveform $R(t; \{T, C_c(t)\})$. The signal s is

Oceans 98 v. 3

therefore convolved with a set of functions that depend upon the unknown parameter sets C_t and C_c associated with the transmitter and channel responses, respectively.

The channel estimator must determine a set of time variant parameters to recover the sequence \mathbf{R} , based on the estimated parameter sets C_t and C_r . The parameter adjustment block processes the signal \mathbf{R} to reproduce the sequence. The received signal $r(t, \mathbf{I}; \mathbf{C})$ is composed of the data \mathbf{R} and the channel parameters \mathbf{C} , which must be jointly estimated. A common method to approach this problem is to send the unknown data sequence separately from a known test sequence in a block structure. The estimator and parameter adjustment elements must operate at a sufficient rate to determine the unknown parameters while they remain quasi-stationary. The link between the parameter set \mathbf{C} and the error rate in \mathbf{R} may be obtained with further definition of the problem.

Assuming the channel is linear, (which may not be the case for wide bandwidth transmissions), the continuous time representation for the signal may be considered as,

$$s(t) = \sum_k a_k h_T(t - kT) e^{j\omega_0 t},$$

where the complex (or amplitude) weighted symbols are designated by a and the transmitter impulse response h_T acts upon symbols delayed in time by integer multiples k of the symbol duration T . The signal exists over a bandwidth B at carrier frequency ω_0 and is subject to multiple influences in both phase and amplitude, which can be expressed as a complex gain factor $h_c(\tau, t)$ that depends upon a delay variable τ and time of observation t . The delay is taken with respect to the first arriving energy packet or, in terms of an acoustic waveguide model, the LOS ray, e.g. τ_p . A set of delay factors τ_n may also be defined to represent separate paths within the waveguide. The *medium* or *channel* impulse response may then be represented by,

$$h_c(\tau, t) \approx \sum_{n=0}^{N-1} h_n(t) \delta(\tau - \tau_p - \tau_n)$$

where the superposition of delay factors is determined by the total number of paths N . The impulse response functions of the transmitter and channel are convolved with the transmitted signal to obtain the received waveform $r(t)$. Measures of τ_{\max} , the maximum delay (*maximum delay spread*) corresponding to τ_{N-1} , may be estimated using a physical model of the channel waveguide and therefore are instrumental in determining the receiver response r :

$$r(t) = e^{j\Omega t} \left\{ \sum_k a_k \sum_{n=0}^{N-1} h_n(t) h_T[(t - kT) - (\tau_p + \tau_n)] \right\} + n(t)$$

$$r(t) = e^{j\Omega t} \left\{ \sum_k a_k h_{\text{eff}}(\tau = t - kT, t) \right\} + n(t)$$

The frequency offset Ω is due to Doppler effects and the

noise $n(t)$ is additive due to ambient conditions. The effective time variant impulse response function $h_{\text{eff}}(\tau, t)$ is as defined above. The complex weighting coefficients of the channel response h_n suggest *phase coherent carrier recovery*, while the differential multipath delays τ_n and timing delays τ_p suggest that *timing synchronization* is required in receiver design.

Over a bandwidth of 20 kHz, the channel exhibits fading and selectivity observed over time, implying variability in h_n . From the previous definitions, the channel response in the frequency domain (capitals) is expressed as the sum:

$$H_{\text{eff}}(\omega, t) = \sum_{n=0}^{N-1} h_n(t) H_T(\omega) e^{-j\omega(\tau_p + \tau_n)}$$

The timing error τ_p is due to propagation and represents the time difference between the arrival of the first signal pulse and the nearest clock pulse of the receiver. The response can be considered flat if the exponential term remains small; that is, when $\omega_{\max} \tau_{\max} \ll 1$. In a band limited channel, the symbol rate can approach half the bandwidth B , so that the requirement becomes $\tau_{\max} \ll T_s$, i.e., the maximum delay in the propagation envelope is much less than the symbol duration. Although this condition implies flatness, fading can also be present through the temporal component of h_n .

The analysis of the response characteristics of the channel can be considered in the time domain, as well as in the τ and ω domains. In particular, fading channels may be categorized according to the temporal duration of the effect, e.g., *long*, *medium*, or *short term*. Modeling of environmental effects on the signal phase and amplitude is highly desirable as it can allow estimation of the long term and medium term temporal characteristics of the channel. Short term modeling requires a scale of resolution that has not been practical to achieve in most communications environments.

The functions characteristically used to describe temporal variability are the delay spread and Doppler spread. The short-term statistics are *completely* characterized by the scattering function, e.g., the *delay-doppler power spectrum* defined as:

$$S(\tau, \psi) = \int_{-\infty}^{\infty} E[h_c(\tau, t) h_c^*(\tau, t + \Delta t)] e^{-j\psi(\Delta t)} d(\Delta t)$$

$$\psi = 2\pi\omega$$

The expected value in this equation is *time delay correlation function* $R_c(\tau, t)$ and ψ is the angular frequency of the Doppler spectra in frequency space ω . The ray weights h_n in this case are statistical processes that can be defined in terms of a set of gain factors α , Doppler shifts ψ_n , and phase shifts θ_n , as follows:

$$h_n(t) = \alpha_n e^{j(\psi_n t + \theta_n)}$$

The parameters in this equation are assumed to be stationary for short intervals, but generally dependent upon time. With this definition under a wide sense stationary uncorrelated statistical (WSSUS) assumption, the scattering function is expressed as:

$$S_c(t, \psi) = \sum_{n=0}^{N-1} \alpha_n^2 \delta(\psi - \psi_n) \delta(\tau - \tau_n)$$

An examination of the Doppler-delay space therefore shows a set of points (τ_n, ψ_n) corresponding to each path in the physical ray model. Points in this space may be considered to be representative of LOS transmission in the absence of internal waves and significant currents. Scattering from surfaces, those are relatively stationary with respect to the source/receiver, produce clusters of points distributed in the τ dimension with little variance in the Doppler space ψ . Specular reflection from moving objects can produce small cluster regions shifted along the ψ -axis. In the one dimensional case, the time delay correlation function may be reduced to the *power delay profile* $R_c(\tau)$ by observing h_c over the same interval ($\Delta t=0$):

$$R_c(\tau, \Delta t = 0) = E[h_c(\tau, t)h_c^*(\tau, t + \Delta t)] = (2\pi)^{-1} \int_{-\infty}^{\infty} S(\tau, \psi)$$

The *delay spread* τ_D , or more appropriately called, the *rms channel delay spread* is the rms value of $R_c(\tau, 0)$. (The *maximum delay spread* was defined previously as $\tau_{\max} = \tau_{N-1} - \tau_0$.) The maximum delay spread is a parameter more suited to receiver design and is preferred. In a similar manner, the *Doppler spread* σ_D is $(2\pi)^{-1} S_c(t=0, \psi)$. The channel *coherence bandwidth* B_c and *coherence time* T_c are approximately the reciprocal of τ_D and σ_D , respectively.

Following the above analysis, the behavior of the communications system is defined in terms of the channel impulse response function, which in turn, may be expressed in physical terms relating to energy propagation in the channel. This approach can provide insight into the effects of the channel on communications performance and establishes the necessary link between physical models of environment and the general communication model. In our research, we are concerned with this association and its use to either improve the performance characteristics of the communication system using model-based forecasts or to establish operational limits based on environmental concerns.

Instead of the simplistic ray model approach expressed in this section, we have chosen to adopt a wave model approach for estimating effects on the channel impulse response. There are both advantages and disadvantages associated with this choice, and indeed the model selection is not unique. Two-dimensional (range-depth) models have been used for initial work due to simplicity and

computational concerns. We have also adopted a *systems identification* approach for adaptive estimation of the channel characteristics because the channel impulse response is obtained directly from the received signal prior to decision making. The approach is therefore that of Fig. 1 where the channel estimator is replaced by a channel model. Advantages obtained include the avoidance of mathematical inversion process necessary with some schemes. Therefore, noise enhancement and stability concerns are relaxed over the *linear equalizer* (LE). In addition, under some circumstances, the delay/stability concerns of the *decision feedback equalizer* (DFE) are avoided.

III. CHANNEL CHARACTERIZATION

Experimental data presented here is derived primarily from offshore tests conducted 5 miles east of the Force Pierce inlet in Florida from October 23 to 25, 1997. The sites of operation were selected for very shallow depths of about 15 meters with a soft-sand substrate. Furthermore, operational range was selected to provide a range-to-depth ratio of over 10, e.g. 600 and 1200 feet. The transmitter was QPSK modulated at 50 kHz, with a bandwidth of 20 kHz. It operated at rates of 5 kBaud and 10 kBaud. The transmitted signal was composed of a 13-element Barker code, a quiet period of 20 symbols, followed by data.

The received signals were successfully decoded using an adaptive equalization with either beamforming or diversity processing. The receiver consisted of a 48-element array and data acquisition system that digitized and recorded all the channels simultaneously. The array was ~2 feet long with hydrophones equally distributed along the length. Sampling at a rate of 800 kHz was followed by decimation, by a factor of 12. The final results were saved for later off-line processing. CTD casts were used to estimate sound speed over the duration of experiment.

Time-varying multipath acoustic propagation was reduced with use of array processing at a carrier-frequency of 50 kHz. The beamwidth between first null (BWFN) using 2, 4 and 10 hydrophone elements was 27.8, 13.8, and 5.5 degrees, respectively.

Figures 2 and 3 show the received signals as a function of the number of channels and distance. The signals start at the beginning of the packet and contain the Barker code, the 20 blank symbols and the data. The results for a distance of 600' show that the multipath dispersion is reduced significantly as the number of beamforming channels is increased. This is expected as beamforming forces the BWFNs to approach the arrival angle for the higher order modes in the channel. For longer distances e.g. 1200' beamforming was less helpful because the surface reflection arrival angle is generally less than the BWFNs of the array. Although there may be an incentive to reduce the BWFN by increasing a number of channels, it should be noted that for larger distances diversity [7]

starts playing an important positive role and the net result improves. In most cases, a *fractionally spaced equalizer (FSE)*, T/2, was used for simulation.

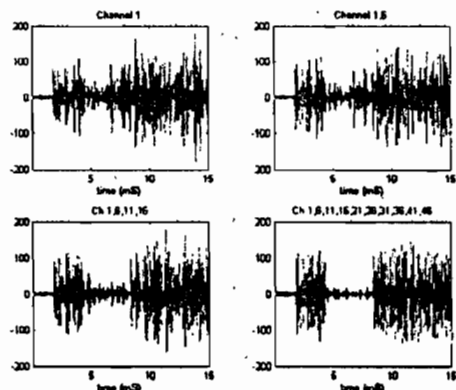


Fig. 2. Beamforming results with 1, 2, 4, and 10 channels at a spacing of 600 feet.

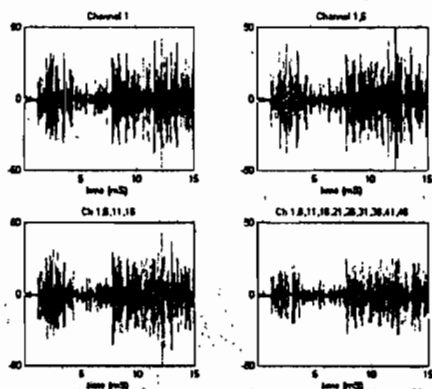


Fig. 3. Beamforming results with 1, 2, 4, and 10 channels at a spacing of 1200 feet.

Processed Experimental Results

Results are strongly a function of the number of channels and separation between transmitter and receiver. At 600 feet, reduced beamwidth corresponding to an increased number of channels, decreases the numbers of errors after equalization. Satisfactory results are obtained when the number of receiver channels, comprising the beamforming elements, is increased to 10. This result is predictable when the first null of the array is smaller than the arrival angle of the surface reflection. For a distance of 1200 feet, some errors occur at the equalizer output even with maximum number of channels. The signal to noise ratio (S/N) of the received signals limits performance at separations over 1200 feet for the projector/receiver pair used. A change in the fractional equalizer from T/2 to T/3 sample period was beneficial. Decoding errors are summarized in Table 1 for various source/receiver separations, number of beam forming elements and data rate.

Distance	kBaud	FSE ¹ [FF,FB] ²	n elements	Errors ³
600 feet	10	T/2 [20,5]	1	370

			2	300
			4	34
			10	0
1200 feet	5	T/2 [10,5]	10	49
		T/3	10	10
	10	T/2	10	32
		T/3	10	6

Table 1: Error Performance, Note: 1. FSE, fractionally spaced equalizer, e.g. T/2, 2 samples per clock.

2. [FE, FB], numbers of the feedforward and feedback taps.

3. Total number of errors from a total of 1000 symbols including 800 decoded symbols and 200 training symbols.

IV. PROPAGATION MODELING

The Monterey-Miami Parabolic Equation (MMPE)[8] was modified and used to model acoustic propagation for changes in environmental conditions. The MMPE travel time option was used to generate the Impulse response (IR) of the acoustic channel. The model defines the time harmonic acoustic field as follows

$$P(r, z, \omega t) = p_{\omega}(r, z)e^{-i\omega t}$$

while the time domain representation of the field is:

$$P(r, z, t) = FFT[p_{\omega}(r, z)] = \sum_{\omega} p_{\omega}(r, z)e^{-i\omega t}$$

The first equation is the single frequency component of the general time dependent field. By choosing a specific frequency, the second equation computes the acoustic field at time $t = 0$. The arrival time structure at some fixed range $r = R$ is computed from the complex field $p_{\omega,R}(z)$ for different frequencies and Fourier transform obtains a set of complex pressure values, $P_R(z, t)$, in time/depth space.

MMPE beamforming

The MMPE model was modified to provide a beamforming option to allow estimation of impulse response. Figure 4 compares the beamformed (BF) and non-beamformed impulse responses (IR). A receiver array at a depth of 10 to 12 m and range of 385 m was used in simulation (water depth~15m). The acoustic wavelength was approximately 40 cm. The single element response follows the beamformed response for the first arrival.

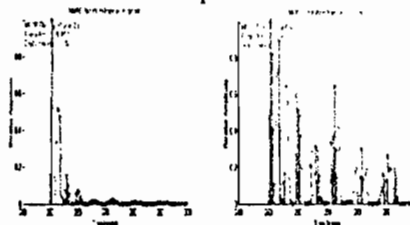


Fig. 4. MMPE IR (Left, BF & 5λ array length, Right, no BF)

Delay spread with motion

The MMPE model representation displays IR delay spread in the range-depth space. A histogram of the total IR

delay spread in the range–depth space and the delay spread for an arbitrary path is shown in Figure 5. The red line denotes the occurrence frequency of particular IR envelope delays and is a measure of the response variability along the path. The path histogram is normalized for the entire range–depth space.

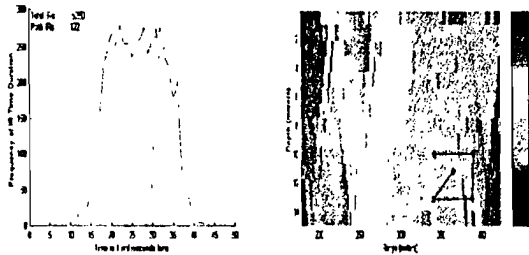


Fig. 5. Right:IR range-depth delay-spread:receiver path outlined in black. Left:histogram of entire range-depth IR delay-spread (blue) and path delay-spread normalized (red).

A comparison of the simulated (resolution 0.5ms) and measured impulse responses (~0.2ms) is given in Fig.6.

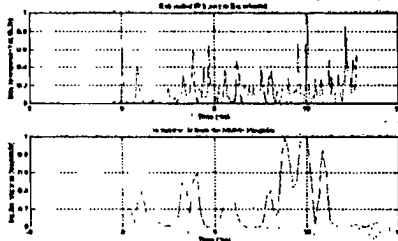


Fig. 6. Comparison of simulated & measured IR(ms)

V. EQUALIZATION WITH SYSTEM ID(EQSID)

The identification of an unknown system is a central issue in the field of control for some time [9,10] and in this context can replace the channel estimator in Fig1 with either a simplified linear model (section II), or an advanced nonlinear or physical model. We use a moving average (MA) model and pass this information to a deconvolutional filter (Parameter Adjustment, Fig. 1) for inverse filtering operation of the received signal. An adaptive algorithm is used to update the model. The EQSID method uses fewer filter coefficients versus other schemes when the channel is temporally variant due to the use an IIR filter for the deconvolutional block. The approach also accommodates non-minimum phase channels [11,12]. A variety of techniques may be used in the implementation for non-minimum phase conditions, including time reversal under specific conditions [13].

The EQSID method is compared to DFE approach for a stationary channel using simulated data and additive gaussian noise as shown in Fig. 7. The convergence was somewhat slower for a given mean square error (MSE) versus the DFE/RLS case. The MSE for the proposed method compares favorably with the results from the DFE case. After convergence, the filter tap weights are directly interpretable according to the impulse response model indicated in Section 2.

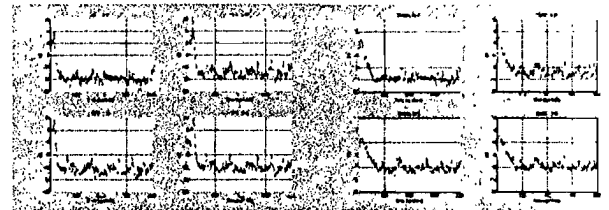


Fig. 7. Comparison of DFE(left) and EQSID (right) mean square error (MSE) vs. iteration number. Channels 1 and 2(top) are minimum phase. Channels 3 and 4(bottom) are non-minimum phase channels. All files: 20 dB SNR.

The computational advantage of the EQSID in relation to other channel estimation methods, e.g. DFE. is good:the number of multiplications per iteration required are $3N+1$, and $2.5N^2+4.5N$, respectively. A comparison of processed data for the beamformed array for $n=1$ (left) and 10(right) are given below for the experimental conditions described.

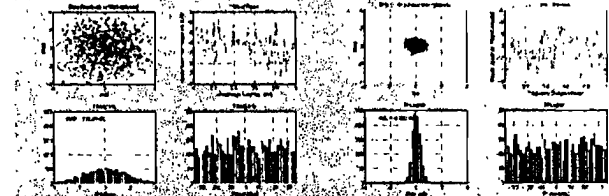


Fig. 8. UL:Error distribution, UR:PSD of amplitude error, LL:Gaussian curve fit to amplitude error histogram(large σ for $n=1$), LR: Histogram of phase error showing uniform distribution.

ACKNOWLEDGMENTS

This research was supported under contract N00014-96-1-5022 under the auspices of Dr. T. Curtin. This paper is Harbor Branch Oceanographic Institution contribution number 1246.

REFERENCES

1. Baggeroer, A.B., "Underwater Acoustic Communications: Introduction," ONR Technology Exchange, Nov. 15, 1997, Arlington, Va.
2. Coates, R., et al. "Underwater Acoustic Communication, A review and Bibliography," Proc. IOA, v.15, 9, 1993.
3. Stojanovic, M. "Recent Advances in High-Speed Underwater Acoustic Communications," IEEE J. Ocean. Eng., vol. 21, no. 2, Apr. 1996.
4. Stojanovic, M., and J. A. Catipovic, and J. G. Proakis, "Phase-Coherent Digital Communications for Underwater Acoustic Channels," IEEE J. Ocean. Eng., vol. 19, no. 1, Jan. 1994.
5. Proakis, J. G., "Adaptive Equalization Techniques for Acoustic Telemetry Channels," III J Oceanic Engineering, 16, 1, Jan. 1991, 21-31.
6. Meyr, H. and R. Subramanian, "Advanced Digital Receiver Principles and Technologies for PCS," IEEE Commun. Magaz., pp 68-78, Jan., 1995.
7. Proakis, J. G., "Digital Communications". New York: McGraw Hill, 1989.
8. Smith, Kevin: Basic Model MMPE Code development, NPGS, 1997.
9. Kalouptsidis, N. and S. Theodoridis, *Adaptive System Identification and Signal Processing Algorithms*, Prentice Hall, 1993.
10. Ljung, *System Identification: Theory for the user*, Prentice Hall, 1987
11. Oppenheim, A.V. and R. W. Schaffer, *Digital Signal Processing*, Englewood Cliffs: Prentice Hall, 1975.
12. Haykin, S. *Adaptive Filter Theory*, 3rd ed., Upper Saddle River: Prentice Hall, 1996.
13. Ariyavisitakul, "A Decision Feedback Equalizer with Time-Reversal Structure," IEEE J. on Selected Areas in Comm., vol. 10, no. 3, Apr. 1992.